LIFT AND DRAG CHARACTERISTICS OF THE M2-F2 LIFTING BODY DURING SUBSONIC GLIDING FLIGHT

by Jon S. Pyle and Robert H. Swanson

Flight Research Center
Edwards, Calif.

CLASSIFICATION CHANGED T

UNCLASSIFIED

1-4-77 per NHB 1640.4B

LIFT AND DRAG CHARACTERISTICS OF THE M2-F2 LIFTING BODY

DURING SUBSONIC GLIDING FLIGHT

By Jon S. Pyle and Robert H. Swanson

Flight Research Center
Edwards, Calif.

GROUP 4
Downgraded at 3 year intervals;
declassified after 12 years

NATIONAL AERONAUTICS AND SPACE ADMINISTRATION

LIFT AND DRAG CHARACTERISTICS OF THE M2-F2 LIFTING BODY

DURING SUBSONIC GLIDING FLIGHT*

By Jon S. Pyle and Robert H. Swanson
Flight Research Center

SUMMARY

The subsonic flight lift and drag characteristics of the M2-F2 lifting-body configuration are presented at angles of attack from -4° to 16°. Flight results are compared with data obtained from full-scale wind-tunnel tests on the flight vehicle.

At an upper-flap deflection of -11.5°, 95 percent of the gear-up (clean airplane) maximum lift-drag ratio (3.13 to 3.16) is available through an angle-of-attack range of 1.5° to 9°. The extension of the landing gear causes a loss of approximately 25 percent in the maximum lift-drag ratio. The gear-up flight and full-scale wind-tunnel maximum lift-drag ratios agree within 3 percent; however, the wind-tunnel data were obtained at a rudder-flare deflection of 0° and the flight results are for a rudder-flare deflection of 5°. The difference between flight and wind-tunnel results would probably be greater than shown if the wind-tunnel data had been adjusted for the 5° flare. The lift coefficients required to attain maximum lift-drag ratios are lower for the gear-up flight results than predicted by the full-scale wind-tunnel tests.

INTRODUCTION

The development of a horizontal landing vehicle that can withstand reentry environments has been the object of extended research. Theoretical and wind-tunnel studies evolved some lifting-body configurations from a series of basic blunt-cone shapes (refs. 1 to 4); however, the basic flight characteristics and landing behavior of these configurations had not been demonstrated. Thus, a manned, lightweight (wing loading of approximately 9 lb/ft^2 (43.9 kg/m^2)) version of the M-2 configuration, designated the M2-F1, was constructed and flight tested (ref. 5) at the NASA Flight Research Center, Edwards, Calif. The M-2 configuration was chosen to demonstrate the flight capabilities of lifting bodies because of the extensive wind-tunnel studies that had been done on this configuration.

As a result of the success of the flight test program of the lightweight vehicle and the need for flight test information on a more representative mission vehicle, a heavier (wing loading of 43 lb/ft^2 (210.2 kg/m^2)) manned version, designated the M2-F2, is being evaluated at the Flight Research Center. The research purpose of these tests is to determine the flight characteristics of the heavier vehicle through the transonic and low supersonic regions as well as at landing speeds. This paper

---

*Title, unclassified.

presents the unpowered subsonic lift and drag characteristics of the M2-F2. Flight data are compared with results from full-scale wind-tunnel tests of the flight vehicle and with M2-F1 flight results.

SYMBOLS

Measurements for this investigation were taken in the U.S. Customary System of Units. Equivalent values are indicated herein in the International System of Units (SI) in the interest of promoting use of this system in future NASA reports. Details concerning the use of SI, together with physical constants and conversions, are given in reference 6.

$\dfrac{A_c}{S}$ nondimensional cross-sectional area

a_l longitudinal acceleration, g

a_n normal acceleration (ratio of net aerodynamic force along airplane Z-axis to weight of airplane), g

b vehicle span, feet (meters)

C_D drag coefficient, $\dfrac{D}{qS}$

$\dfrac{\Delta C_D}{\Delta C_L{}^2}$ drag-due-to-lift factor

C_L lift coefficient, $\dfrac{L}{qS}$

C_{L_α} lift-curve slope, degree^{-1}

C_N normal-force coefficient, $\dfrac{Wa_n}{qS}$

C_X axial-force coefficient, $\dfrac{Wa_l}{qS}$

D drag force along flight path, pounds (newtons)

$\dfrac{d}{l}$ ratio of distance from nose of M2-F2 to an arbitrary point along horizontal reference line and total M2-F2 length, percent

g gravitational acceleration, 32.2 feet/second^2 (9.8 meters/second^2)

h	altitude of vehicle above touchdown point, feet (meters)
L	lift force normal to flight path, pounds (newtons)
$\dfrac{L}{D}$	lift-drag ratio
M	free-stream Mach number
M$'$	indicated Mach number
ΔM	Mach number error, M $-$ M$'$
p	corrected static pressure, pounds/foot^2 (newtons/meter^2)
p$'$	indicated static pressure (from nose boom), pounds/foot^2 (newtons/meter^2)
Δp	position error in static pressure, p$'$ $-$ p, pounds/foot^2 (newtons/meter^2)
q	dynamic pressure, pounds/foot^2 (newtons/meter^2)
S	reference body area, 139 feet^2 (12.9 meters^2)
W	vehicle weight, pounds (kilograms)
x	longitudinal distance of vehicle from touchdown point, feet (meters)
y	lateral distance of vehicle from touchdown point, feet (meters)
α	corrected angle of attack, degrees
α'	adjusted angle of attack, $\alpha_m + \Delta\alpha_\beta + \Delta\alpha_q + \Delta\alpha_\epsilon$, degrees
α_m	measured angle of attack, degrees
$\Delta\alpha_q$	angle-of-attack correction for pitching rates on angle-of-attack vane, degrees
$\Delta\alpha_\beta$	angle-of-attack correction for nose-boom bending due to normal forces, degrees
$\Delta\alpha_\epsilon$	angle-of-attack correction for upwash factor with Mach number, degrees
δ	flap deflection, degrees
σ	root-mean-squared error

Subscripts:

lf lower flap

max   maximum

min   minimum

uf   upper flaps

VEHICLE DESCRIPTION

The M2-F2 is a wingless, lifting configuration constructed primarily of aluminum. The structure incorporates a semimonocoque construction technique with two full-depth keels. The configuration has a basic half-cone shape with blunted nose and boattailed afterbody. Table I presents the pertinent physical characteristics of the vehicle. Photographs of the vehicle with the landing gear stowed and extended are shown in figures 1(a) and 1(b), respectively.
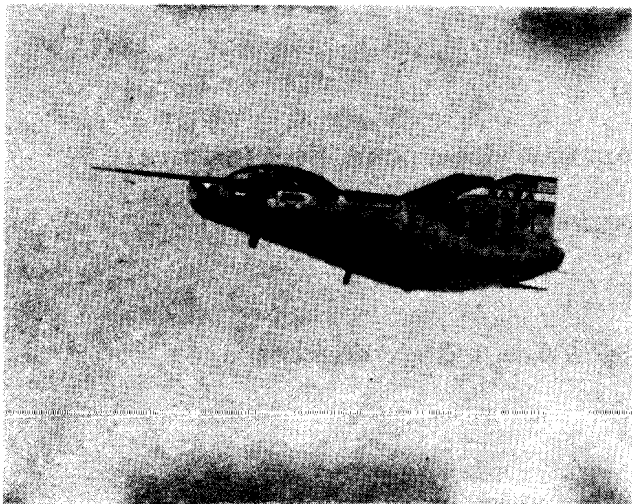
E-16467

(a) Gear up.
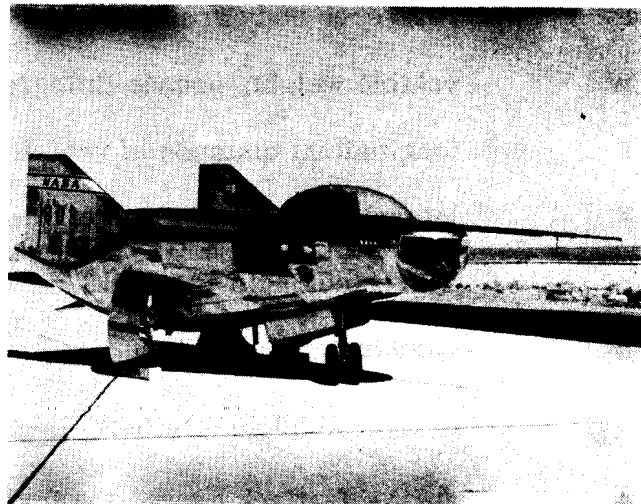
E-14332

(b) Gear down.

Figure 1.— M2-F2 configuration.

Figure 2 presents the variation of the nondimensional cross-sectional area of the M2-F2 vehicle with percent of body length. The reference area of 139 feet^2 (12.9 meters^2) used throughout this paper was obtained from the basic M-2 configuration body planform area and has been used as a basis of comparison for various M-2 configurations since their inception by the Ames Research Center. The coefficient data presented herein may be converted to the actual body planform area (160 feet^2 (14.9 meters^2)) by using the conversion factor of 0.869.
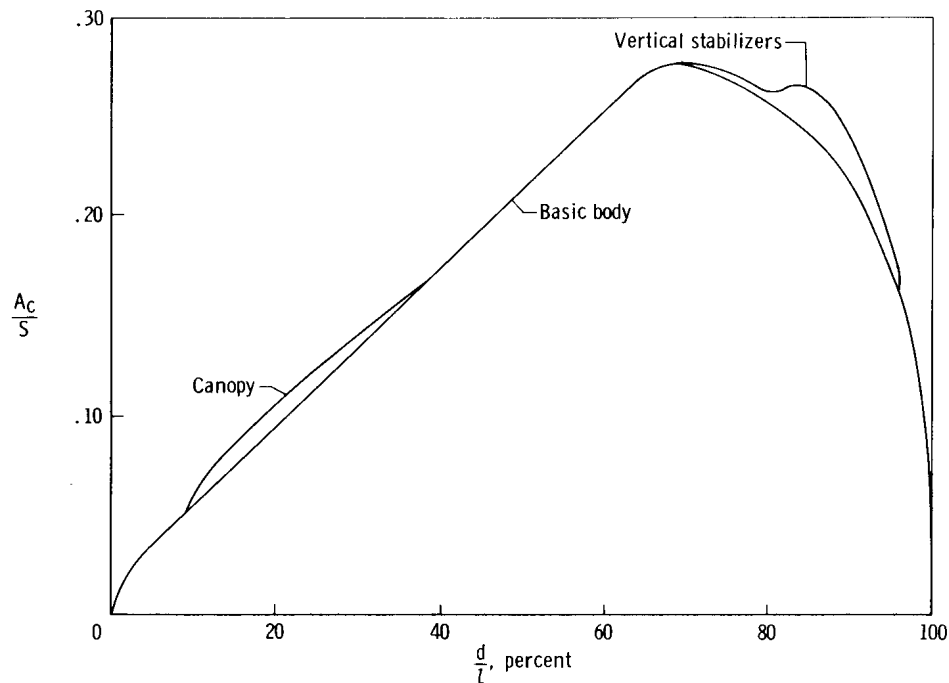

4

Figure 2.— M2-F2 area distribution.

The M2-F2 upper flaps and the lower flap were built into the aft portion of the vehicle body (fig. 3) and are at 0° deflection when tangent to the body contours. Space was provided below the upper flap for asymmetric deflections as much as 10° below the body contour. The rudders were built into the outboard, rear portion of the vertical stabilizers and can be deflected outward only. Extendable landing gear were included to simulate the performance of an actual mission vehicle. During flight, the nose and main landing gear are contained in recessed cavities within the hull of the vehicle. In the gear-down configuration the gear doors and wheels are extended, exposing the large wheel-well cavities to the airstream. The movable portion of the gear doors (nose and main gear) represents a total area of 23.87 feet^2 (2.217 meters^2). The total volume of the wheel-well cavities is 23.03 feet^3 (0.652 meter^3). The position of the doors and of the wheel-well cavities can be seen in figure 1(b).
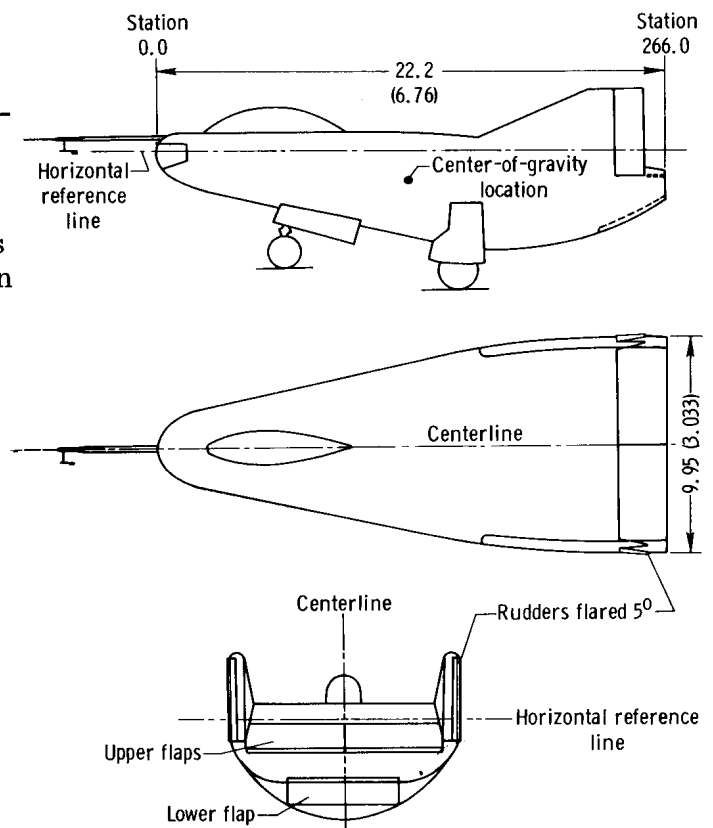

Figure 3.— Three-view drawing of the M2-F2 configuration. All dimensions in feet (meters).

5

The gear on a mission vehicle could be optimized to provide less drag than was experienced with the M2-F2. Also, since the M2-F2 vehicle has a standard production aluminum surface, the lift and drag results presented are not characteristic of a mission vehicle with a post-entry surface of charred ablatives.

The primary longitudinal control surface for the M2-F2 vehicle is the lower flap, which is controlled through the control stick. Longitudinal trim is obtained by means of the upper flaps and is controlled by a trim wheel in the cockpit. A constant deflection for the upper flap is set before launch, and longitudinal control is maintained throughout the flight by means of the lower flap. When the upper flaps are deflected symmetrically upward for longitudinal control (indicated by an increase in negative deflection), the lower flap must be deflected downward (indicated by an increase in positive deflection) to keep the vehicle trimmed. As the vehicle is trimmed with any upper-flap setting, the control surfaces (upper and lower flaps) alter the boattailed afterbody into a wedge shape (fig. 4(a)). Lateral control is obtained through asymmetric deflection of the upper flaps and is controlled through the control stick.

The M2-F2 controls include dual rudders for directional control (fig. 4(b)). These surfaces can be flared to any neutral position by ground adjustment. Because of the excessive adverse yaw due to aileron deflection, a rudder interconnect was provided. The ratio of rudder to aileron is mechanically adjustable by the pilot in the cockpit. The roll stability augmentation system operates through the interconnect of the rudders and the ailerons.
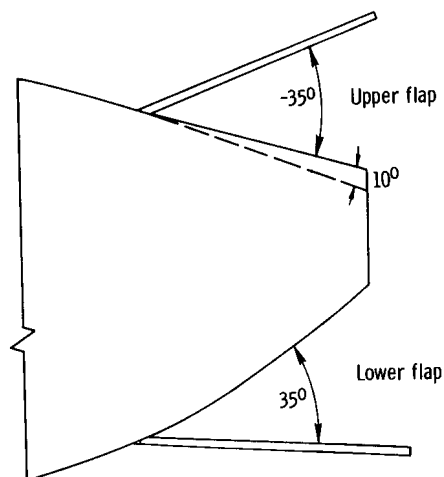
(a) Side view (cutaway) showing upper- and lower-flap deflections and wedge effect.
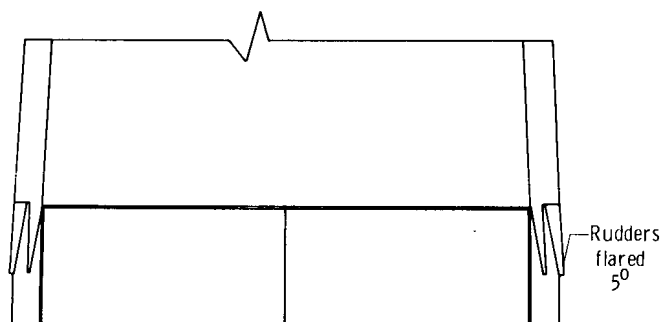
(b) Top-view showing 5° rudder flare.

Figure 4.— Sketches of the aft portion of the M2-F2 vehicle showing control-surface travel.

The wing loading was approximately 43 lb/ft^2 (210.2 kg/m^2) based on the reference area of 139 feet^2 (12.9 meters^2). The center of gravity for the flight tests was at approximately 49 percent of the total vehicle length of 22.2 feet (6.76 meters).

Flight Tests

The glide flights of the M2-F2 lifting body were made after launch from a B-52 airplane at an altitude of about 44,000 feet (13,400 meters) and an average Mach number of 0.63. After approximately 3 minutes of free gliding flight, the landing maneuver was completed on Rogers Dry Lake. The ground track and altitude loss during a typical flight are shown in figure 5. The ground track shows the lateral and longitudinal distance of the vehicle from the touchdown point. The values of Mach number and dynamic pressure are indicated at various positions along the ground track. Corresponding altitudes are presented with longitudinal distance from touchdown to give an indication of the altitude loss during the flight. Because of the relatively short duration of the flight, the time for maneuvering the vehicle was limited. However, the pilots were able to perform adequate push-over/pullup maneuvers and banked turns to define the lift and drag characteristics of the vehicle. The data presented herein were obtained from 10 flights flown by four different pilots.

Landing techniques used for the M2-F2 were the same as those developed for the X-15 aircraft (ref. 7). Deployment of the gear was delayed until the landing flare was completed and the vehicle was close to the ground. Data obtained after gear deployment were subject to ground effect and the transient, untrimmed conditions caused by the deployment.

All M2-F2 data presented in this paper were obtained at altitudes below 45,000 feet (13,700 meters) and at Mach numbers from 0.25 to 0.64. Angle of attack varied from -4° to 16°. Reynolds numbers for the flight tests ranged from 16×10^6 to 55×10^6, based on a body length of 22.2 feet (6.76 meters). The upper flaps were
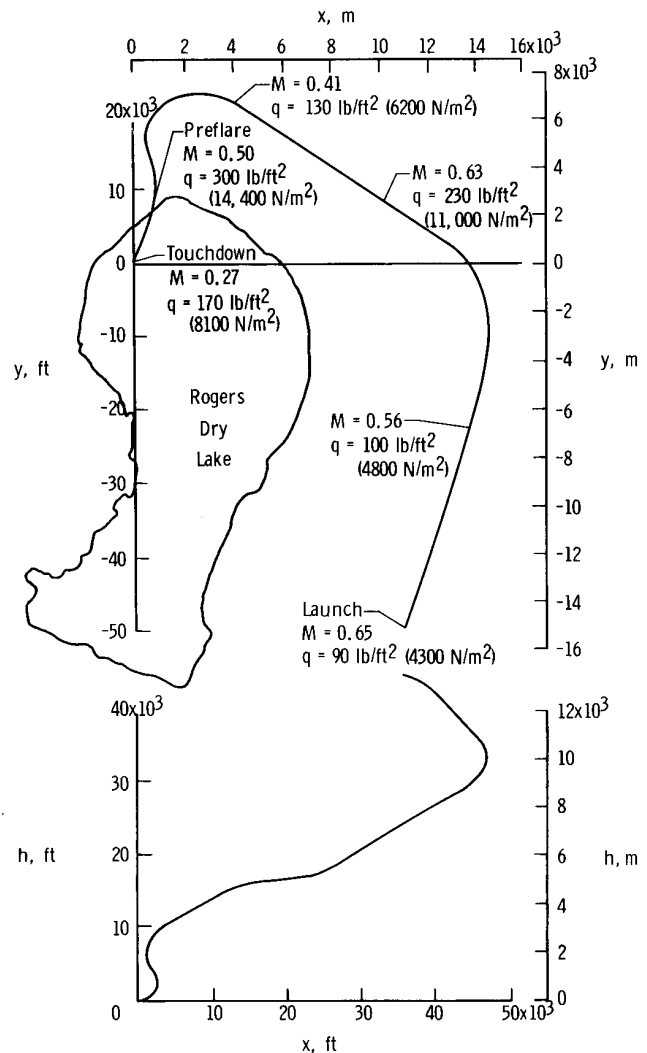

Figure 5.— Ground and altitude tracks for the M2-F2 vehicle during a typical glide flight.

7

deflected at -11.5° for all maneuvers except two, which were performed at deflections of -8.5° and -14.5°. The rudders were mechanically trimmed for 5° of flare.
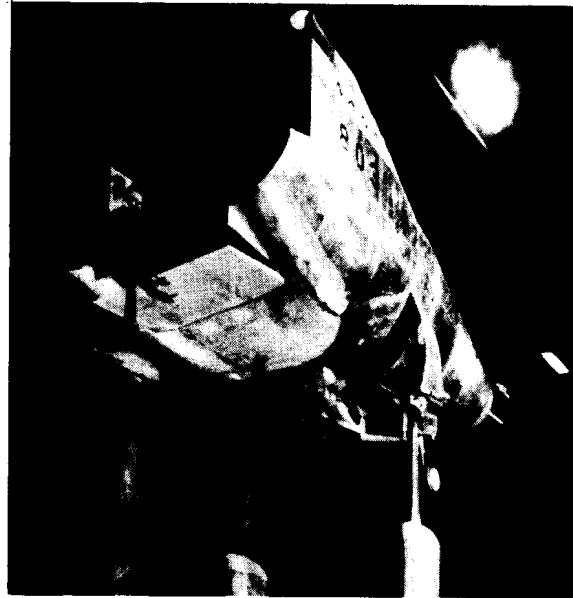
Wind-Tunnel Tests

Before flight tests of the M2-F2 lifting body, wind-tunnel tests were conducted on the flight vehicle in the Ames 40- by 80-foot wind tunnel. Photographs taken during the tests in the full-scale tunnel are shown in figure 6(a) and figure 6(b).
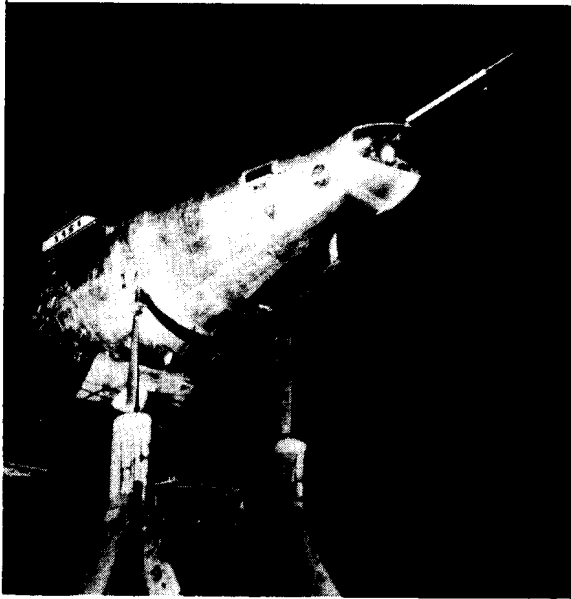
E-13742

(a) Gear up.

E-13743

(b) Gear down.

Figure 6.— M2-F2 configuration mounted in the full-scale wind tunnel.

The wind-tunnel data were faired and trimmed about the in-flight center-of-gravity position and then interpolated to an upper-flap deflection of -11.5° for comparison with the flight results.

Although the rudders were set for flight, symmetrically neutralized, at 5° of rudder flare, most of the wind-tunnel data represent 0° rudder flare. The wind-tunnel drag curves could not be corrected to flight conditions because of the limited amount of 5° rudder-flare data. However, enough 5° rudder-flare wind-tunnel data were available to obtain an increment of drag (at a constant lift-coefficient value) resulting from the change in rudder-flare position. This increment is discussed quantitatively in the DISCUSSION section.

The full-scale wind-tunnel tests were conducted at Mach numbers from 0.15 to 0.25. Angle of attack varied from -10° to 30°. Reynolds numbers for the tests ranged from 22×10^6 to 41×10^6, based on a body length of 22.2 feet (6.76 meters).

INSTRUMENTATION

Description

The accelerations of the M2-F2 vehicle were measured by sensitive accelerometers mounted as close to the vehicle's center of gravity as possible. The corrections to the measurements necessitated by the displacement of the accelerometers were neglected because of their small magnitudes. A standard NACA nose boom was used to measure static pressure, differential pressure, angle of attack, and angle of sideslip (ref. 8). The angle of attack was measured by a floating vane positioned 3.95 feet (1.204 meters) forward of the vehicle nose. The static- and total-pressure orifices were 5.59 feet (1.704 meters) and 6.25 feet (1.905 meters), respectively, forward of the M2-F2 nose. All data obtained from the onboard instrumentation were telemetered to ground stations by using a pulse code modulation system. The techniques used to determine lift and drag are discussed in reference 9.

Special Calibrations

Angle of attack.— The angle-of-attack vane was calibrated in the full-scale wind tunnel (fig. 7) through a range of -10° to 30°. The least-squares analysis of the data scatter indicates approximately ±0.7° standard error estimate (68 percent of data scatter within this error band).
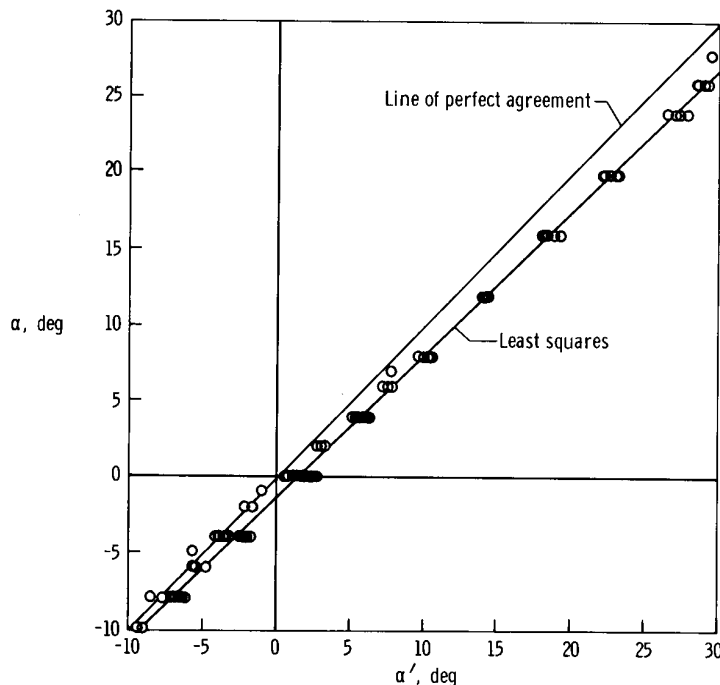

Figure 7.— Full-scale wind-tunnel angle-of-attack calibrations for the M2-F2 vehicle. M = 0.2.

The total upwash (body and nose boom, $\dfrac{\Delta\alpha_\epsilon}{\alpha_m}$) of the angle-of-attack vane at a Mach number of 0.2 was estimated from the full-scale wind-tunnel tests and is presented in figure 8 as a circular symbol. In order to obtain a correction for total upwash on the angle-of-attack vane through the subsonic Mach number region, several calculations were made with the dimensions of the M2-F2 nose-boom and body configurations using the methods of reference 10. The calculated nose-boom upwash is shown as a dashed line in figure 8. The body-upwash effect was more difficult to calculate because of its asymmetric shape. Several attempts to calculate the body upwash were made by using equivalent bodies of revolution generated individually by the top, bottom, and side contours. Poor correlation was evident when these calculations were added individually to the calculated nose-boom upwash effect and compared to the estimated wind-tunnel upwash on the angle-of-attack vane; therefore, the calculations were discarded. An additional calculation was made using the radii obtained from the M2-F2 area distribution (fig. 2) converted to an equivalent body of revolution. The calculation when added to the nose-boom upwash (solid line) agreed closely with the estimated total upwash obtained from the wind-tunnel results. The difference between the wind-tunnel total-upwash factor and the calculated total upwash factor (at its associated Mach number) is the correction to the measured angle of attack $\Delta\alpha_\epsilon$.
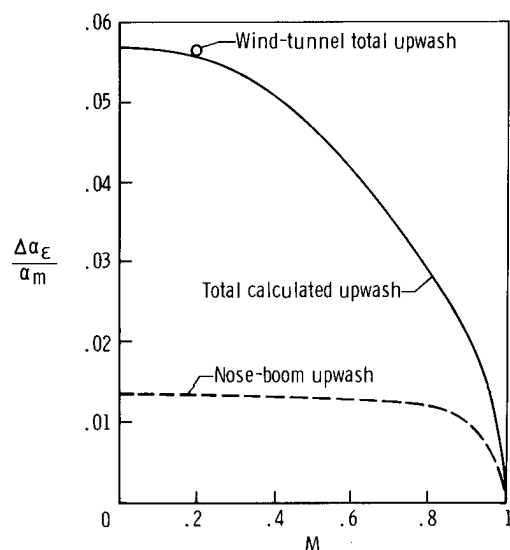

Figure 8.— Calculated upwash factor for the angle-of-attack vane.

The angle-of-attack vane was calibrated for the effect of boom bending $\Delta\alpha_\beta$ due to normal accelerations, and the flight data were corrected accordingly. A correction for pitching rate $\Delta\alpha_q$ on the angle-of-attack vane (15.55 feet (4.740 meters) forward of the vehicle's center of gravity) was also made to the measured angle of attack. The total corrections that were made to the measured angle of attack to obtain the adjusted angle of attack were as follows:

(1) $\alpha' = \alpha_m + \Delta\alpha_\beta + \Delta\alpha_q + \Delta\alpha_\epsilon$

(2) α' converted to α by means of the wind-tunnel calibration shown in figure 7

Air data measurements. — The nose boom was calibrated for static pressure and Mach number position error by using the radiosonde balloon and radar method of reference 11. The relationship of ambient pressure with altitude (as defined by radar) was obtained from radiosonde balloon measurements by using the hydrostatic equation. The relationship of the onboard-measured static pressure to ambient pressure was established by comparing the radar-defined altitudes of the aircraft and the radiosonde balloon. The calibration of position error as a function of indicated Mach number is shown in figures 9(a) and 9(b).

(a) Static-pressure error; $p = \dfrac{p'}{\left(1 + \dfrac{\Delta p}{p}\right)}$.
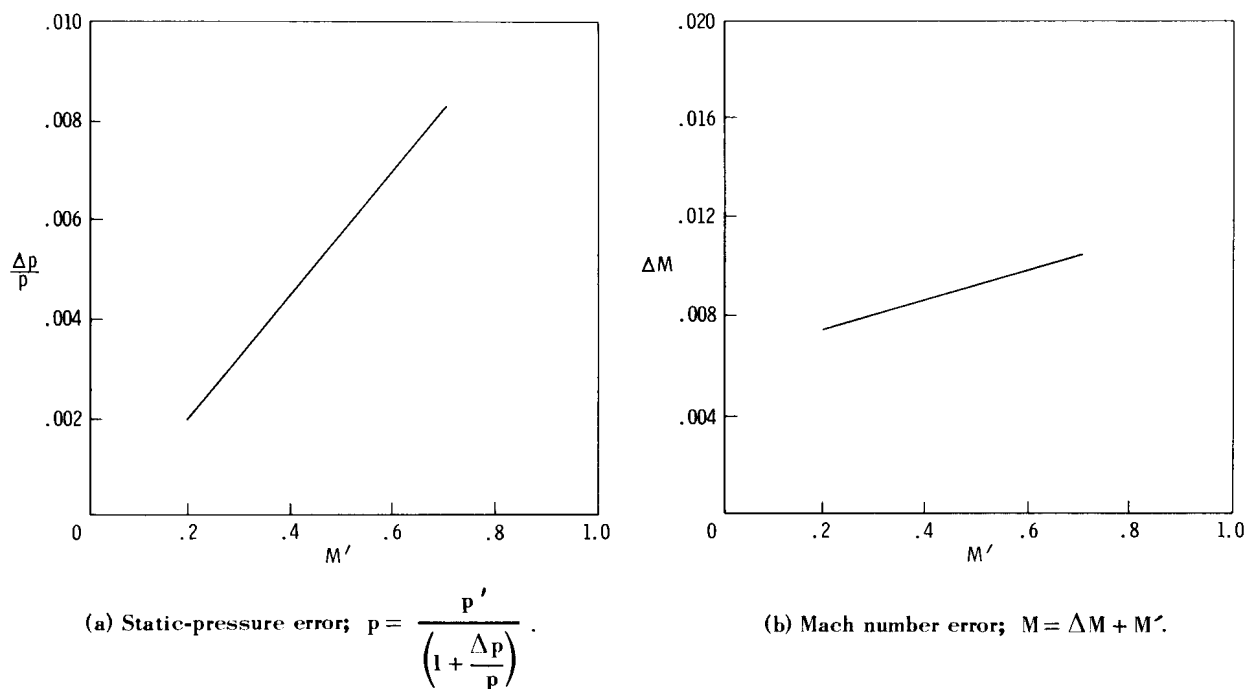
(b) Mach number error; $M = \Delta M + M'$.

Figure 9.— Position error of the airspeed system used on the M2-F2.

METHOD OF MEASUREMENT

Measurements of normal and axial accelerations were used in the determination of lift and drag. The development of the equations used in this method is presented in reference 9. The following relationships apply to the data presented herein:

$$C_L = C_N \cos \alpha - C_X \sin \alpha$$

$$C_D = C_X \cos \alpha + C_N \sin \alpha$$

ERRORS AND RELIABILITY

The standard deviation of the errors for the measurements, which include instrument, transmission, and data-reduction systems, was as follows:

|	
W, pounds (kilograms)	±5 (±2.3)
a_n, g	±0.013
a_l, g	±0.003
q, lb/ft^2 (N/m^2)	±1.80 (±86.2)
α, degrees	±0.5
M	±0.01

Examination of these quantities individually indicates the types of errors that occur in measurements of lift and drag. Although the errors inherent in the measurement of weight are biased for each flight, the biased errors should become random when data from several flights are used. The individual measurement errors of the accelerometers, airspeed (q and M), and angle of attack are random. The biased errors that may occur in these quantities are reduced by careful calibrations, correction of zero shifts, and proper location of the instruments within the aircraft. Therefore, since most of the errors are random, the fairings of flight data reduce the net error significantly. The errors caused by extreme transient pitch motions were reduced by limiting pitch rates to within ±5 degrees/second for the gear-up and the gear-down flight data.

The net random error involved in the measurement of lift and drag was best represented by the root-mean-squared algebraic summation of the random errors. The effect of each error in the evaluation of lift coefficient, drag coefficient, and lift-drag ratio is shown in the following table. These errors represent data at the maximum gear-up lift-drag ratio of 3.16 and at a Mach number of 0.4.

|	$\dfrac{\sigma C_L}{C_L}$, percent	$\dfrac{\sigma C_D}{C_D}$, percent	$\dfrac{\sigma \frac{L}{D}}{\frac{L}{D}}$, percent
W	±0.8	±0.8	----
a_n	±1.0	±0.2	Negligible
a_l	Negligible	±0.8	Negligible
q	±1.0	±1.0	----
α	±0.3	±2.8	±3.0
σ	±1.5 %	±3.0 %	±3.0 %

DISCUSSION

The subsonic flight lift curves, drag polars, and lift-drag ratios obtained on the M2-F2 vehicle are presented in figures 10, 11, and 12, respectively. These figures indicate the data scatter for the large number of data points used in obtaining the gear-up and gear-down faired flight results that are presented in the following discussion. The gear-up data were obtained at Mach numbers from 0.42 to 0.50 and 0.60 to 0.64 (presented as nominal values of 0.45 and 0.64, respectively). The gear-down flight results were obtained at Mach numbers from 0.24 to 0.35 (presented as a nominal value of 0.3).
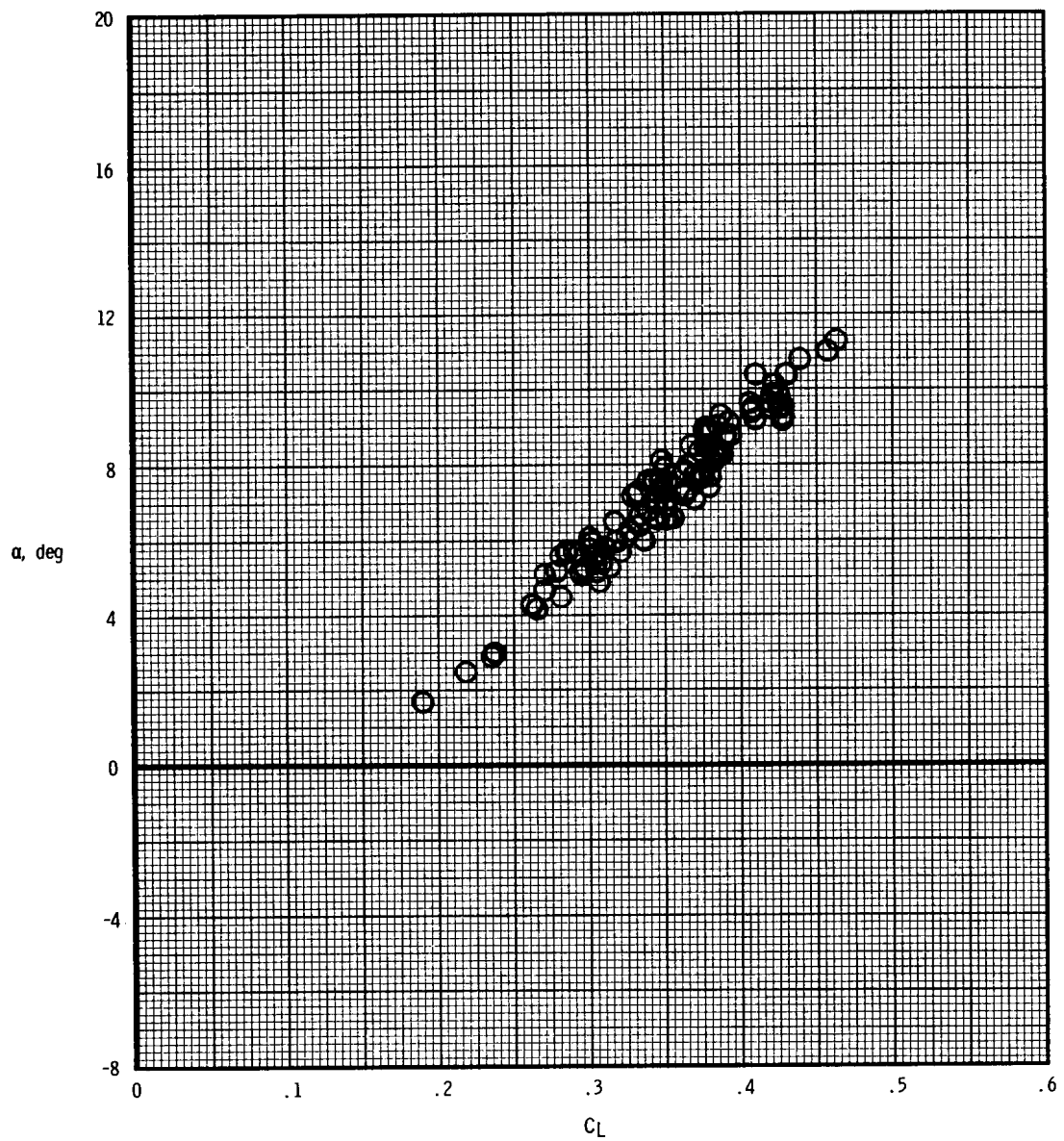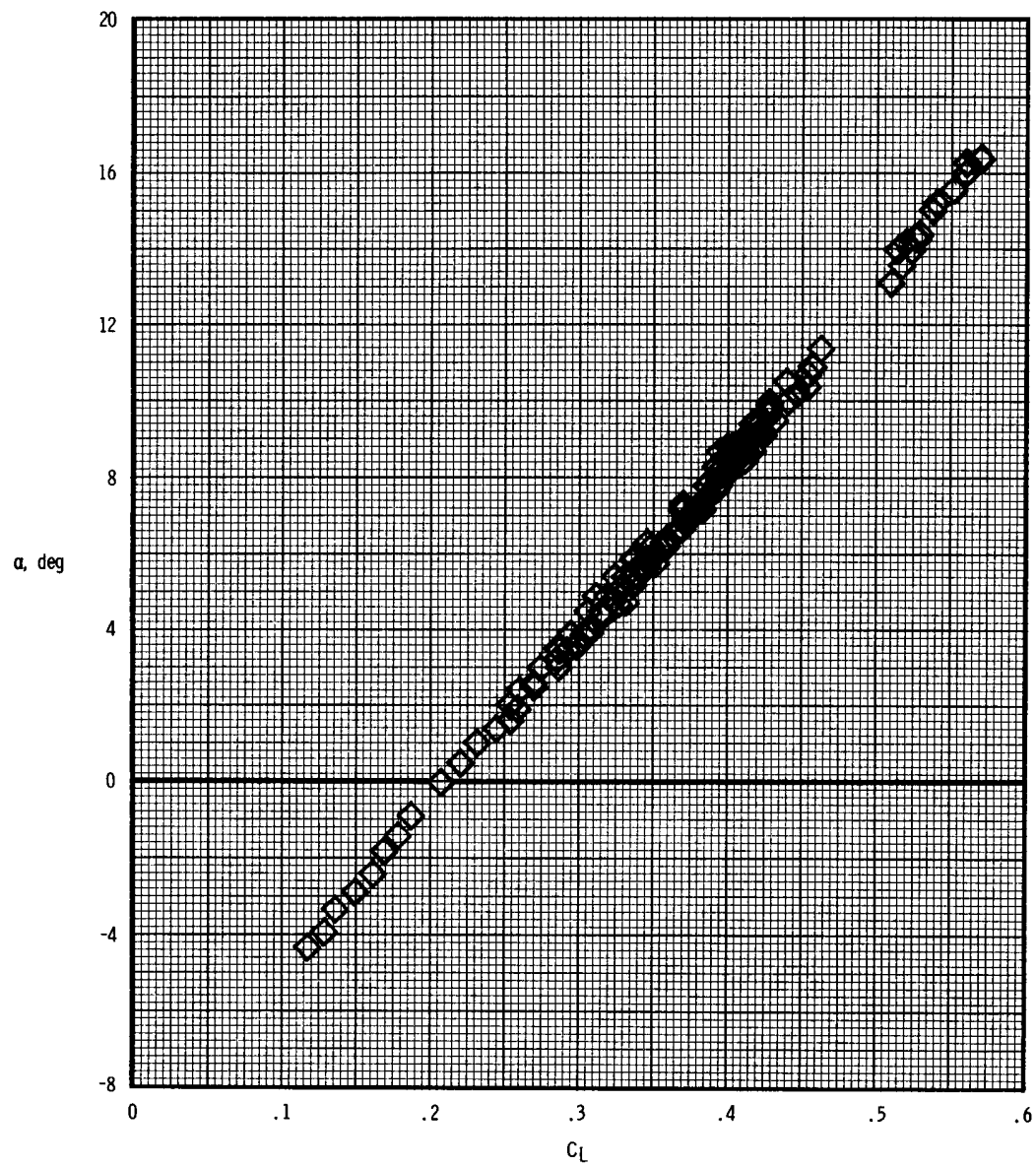
(a) Gear down, M = 0.3.

Figure 10.— Flight-measured lift curves for the M2-F2 configuration. $\delta_{uf} = -11.5^{\circ}$.
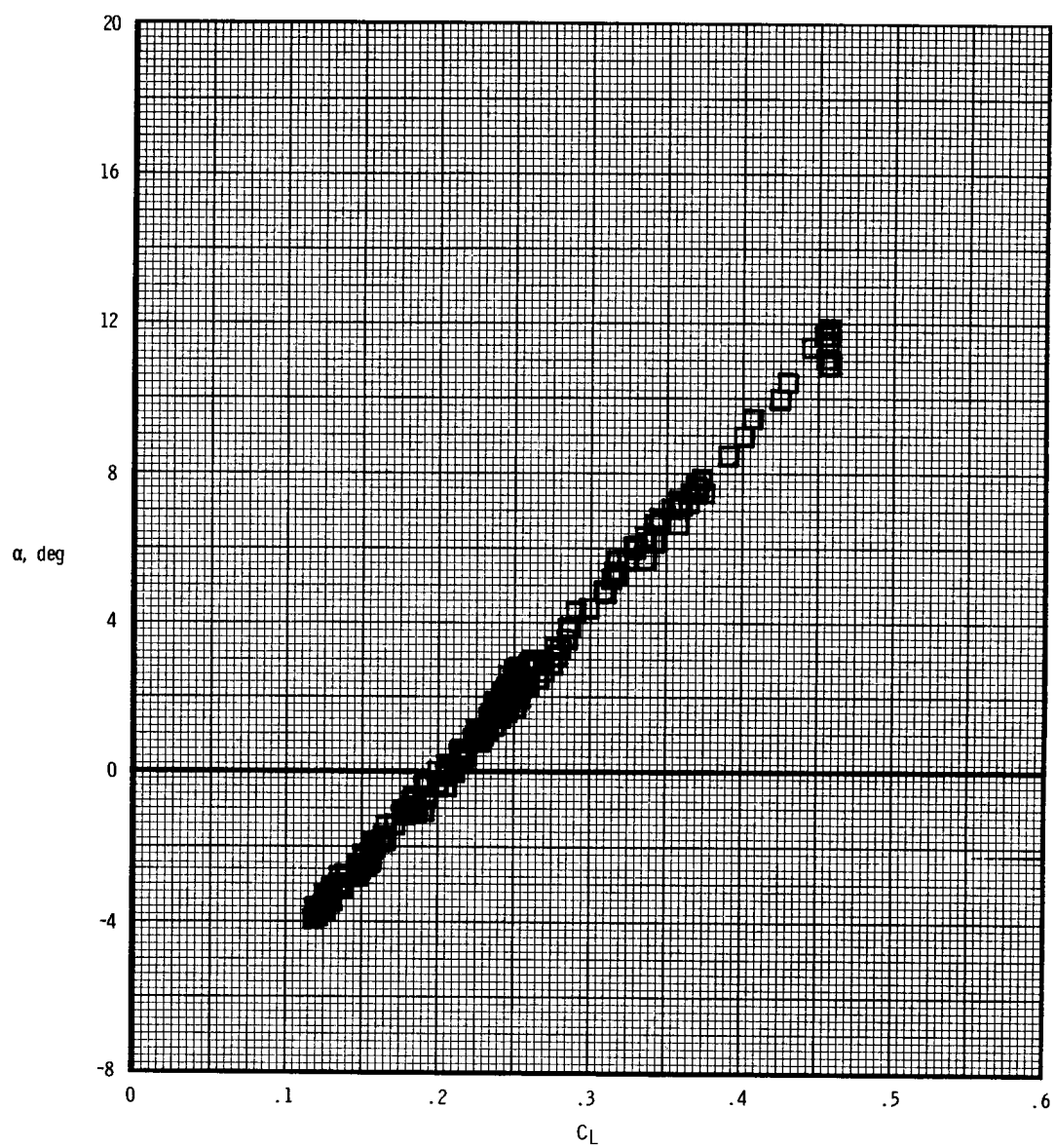
(b) Gear up, M = 0.45.

Figure 10.— Continued.
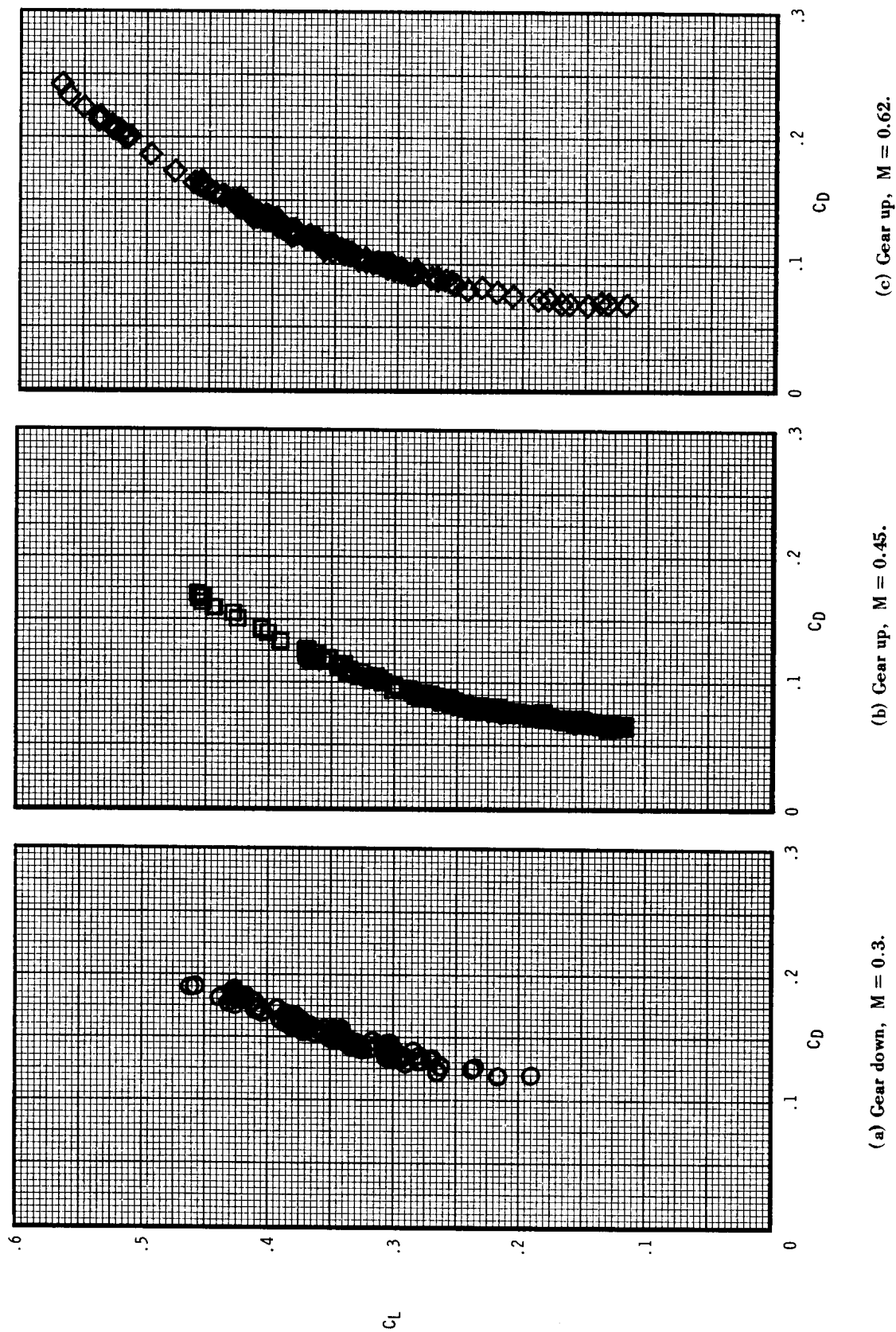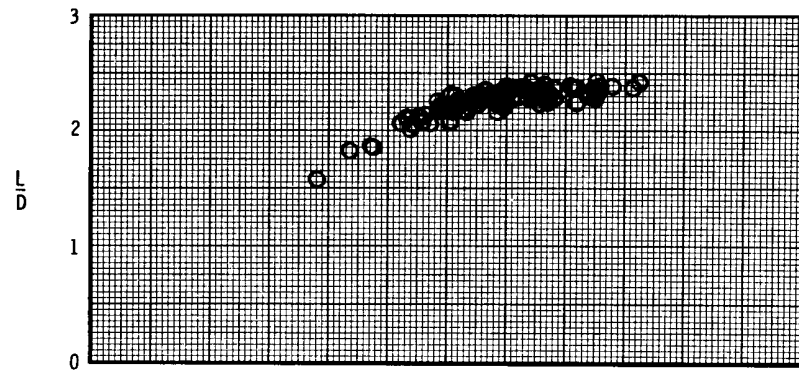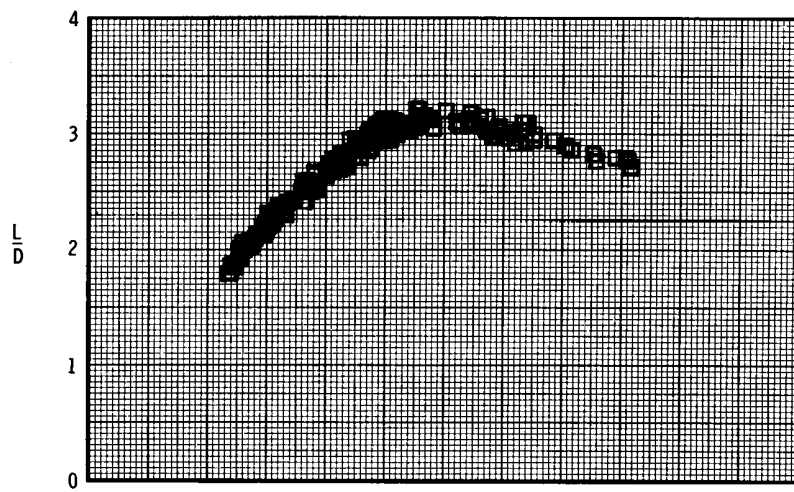
14

(c) Gear up, M = 0.62.

Figure 10.— Concluded.

(a) Gear down, M = 0.3.

(b) Gear up, M = 0.45.

(c) Gear up, M = 0.62.

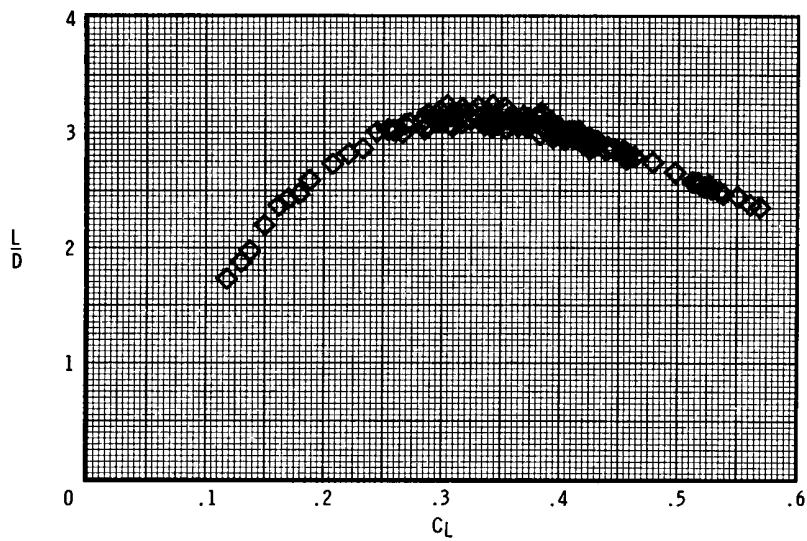Figure 11.— Drag polars obtained for the M2-F2 from subsonic flight. $\delta_{uf} = -11.5°$.

(a) Gear down, M = 0.3.

(b) Gear up, M = 0.45.

(c) Gear up, M = 0.62.

Figure 12.— M2-F2 lift-drag-ratio data determined from subsonic flight. $\delta_{uf} = -11.5^{\circ}$.

The full-scale wind-tunnel results, from tests on the flight vehicle, were obtained at Mach numbers from 0.15 to 0.25 (presented as M = 0.2) and are compared with the subsonic gliding flight results. Some of the differences between the flight and full-scale wind-tunnel results may have been caused by interference between the wind-tunnel mounts and the flight vehicle. The limited number of wind-tunnel trim points available for interpolating the wind-tunnel data to flight conditions may have caused additional, though small, errors. These full-scale data, rather than small-scale wind-tunnel results, were chosen for comparison with flight results because of the simulation deficiencies inherent in the available small-scale wind-tunnel data. The small-scale model that most nearly represented the M2-F2 flight vehicle had an open base and a hollow body. The small models were also subject to sting interference effects.

The variation of angle of attack with lower-flap deflection is shown in figure 13. The flight data presented were obtained from the points used for the calculation of the lift and drag characteristics and, therefore, do not represent the actual trim curves of the M2-F2 vehicle under steady-state conditions. However, full-scale wind-tunnel curves are presented for comparison with gear-up flight data. A slight change in slope between the flight and wind-tunnel results is evident, especially at M = 0.45 where the results differ slightly in magnitude. A slope for the gear-down flight data could not be determined because of the difficulties encountered in attaining trimmed conditions between gear deployment and touchdown. Additional scatter in the
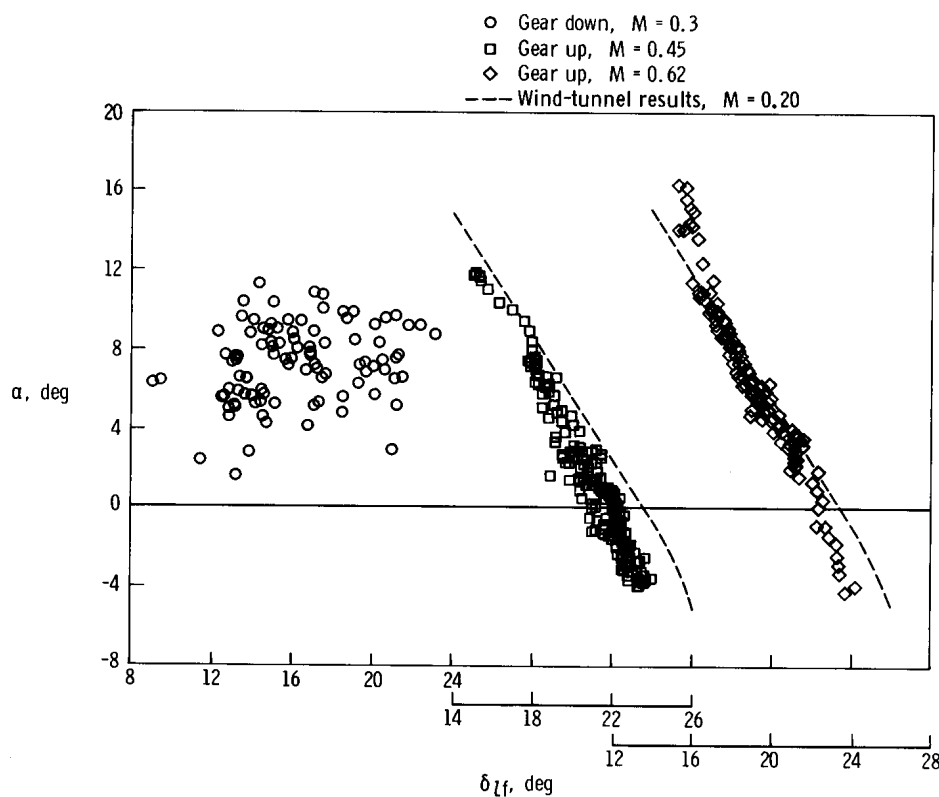

Figure 13.— Variation of angle of attack with lower-flap deflection obtained from M2-F2 results. $\delta_{uf} = -11.5°$.

gear-down flight data may be due to the
presence of ground effects on the vehicle
prior to touchdown. Although the aircraft
was untrimmed while most of the gear-
down data were being obtained, it was
possible to calculate the lift and drag
characteristics. These characteristics
are compared with trimmed full-scale
wind-tunnel results.

Lift Characteristics

Faired M2-F2 flight results are
compared with full-scale wind-tunnel
results in figure 14. The flight-
determined lift-curve slopes for the
gear-up configuration indicate negligi-
ble effect of Mach number over the
range tested, although the results show
a slight shift in lift coefficient at a
given angle of attack between the
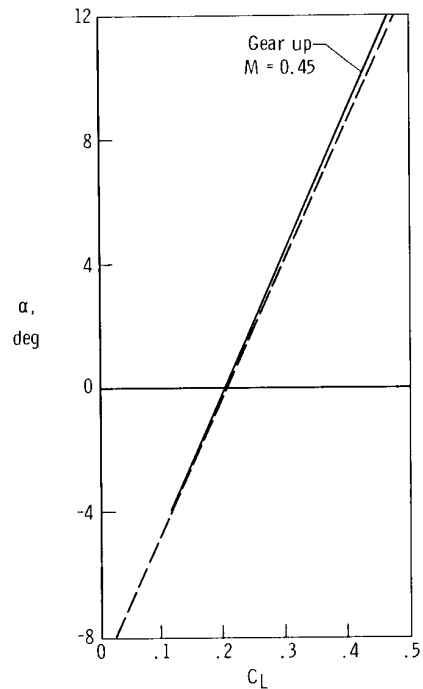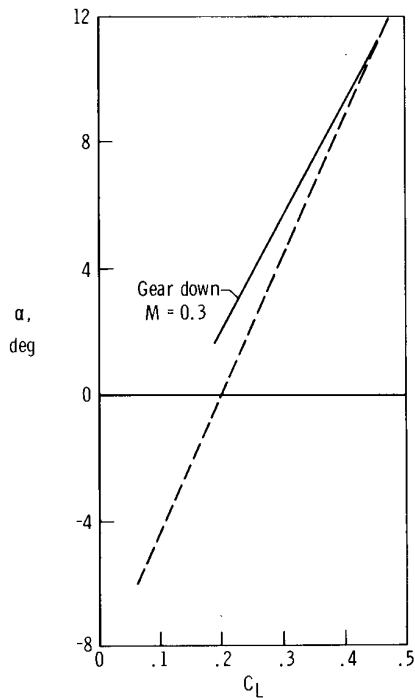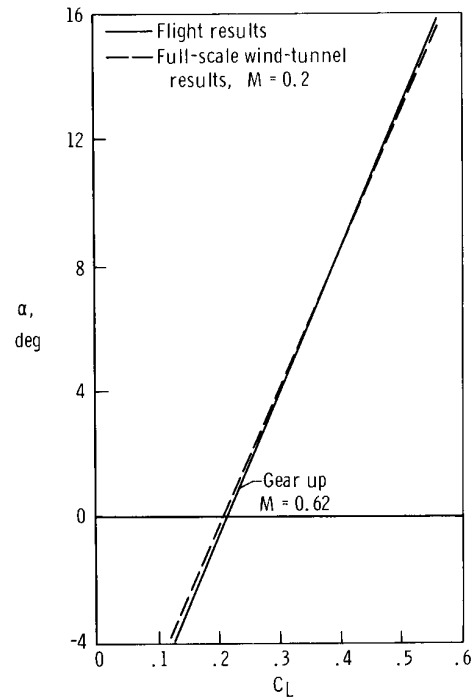$M = 0.45$ and $M = 0.62$ data.

Figure 14.— Comparison of faired M2-F2 lift curves with full-scale wind-tunnel
results. $\delta_{uf} = -11.5^\circ$.

19

Lift-curve slopes obtained from the preceding figure are compared in the following table:

	Gear down		Gear up		
	Flight, M = 0.3	Wind tunnel, M = 0.2	Flight, M = 0.45	Flight, M = 0.62	Wind tunnel, M = 0.2
C_{L_α}, degree^{-1}	0.0277	0.0227	0.0217	0.0216	0.0225
$\dfrac{1}{C_{L_\alpha}}$, radian*	0.630	0.769	0.804	0.808	0.776

The gear-up flight C_{L_α} values are approximately 5 percent less than those obtained

from the wind-tunnel results. The gear-down flight results show the opposite trend, indicating approximately 18 percent greater slope than the full-scale wind-tunnel data. This may be an additional indication of the presence of ground effect mentioned previously.

Drag Characteristics

The M2-F2 flight drag results (faired from data curves of fig. 11) are shown with full-scale wind-tunnel data in figure 15. The comparison of the gear-up drag polars obtained from flight data indicates negligible effect of Mach number. The gear-up flight results show a greater drag-due-to-lift than the full-scale wind-tunnel results. The gear-down flight and wind-tunnel data are similar in magnitude where data were available.

The inability to obtain interpolated wind-tunnel results at 5° rudder flare for comparison with flight results was mentioned previously (page 8). However, an increment of drag (0.005 at C_L = 0.2) was obtained from comparable wind-tunnel results at

rudder-flare deflections of 0° and 5°. This increment is presented in figure 15 (M = 0.45) to indicate the probable change in the wind-tunnel drag polar if adequate data were available for interpolating. If the data were available, the difference between

---

*Although more significant at higher Mach numbers, $\dfrac{1}{C_{L_\alpha}}$ is included to enable

comparison with $\dfrac{\Delta C_D}{\Delta C_L{}^2}$, which is shown in the table on page 22.
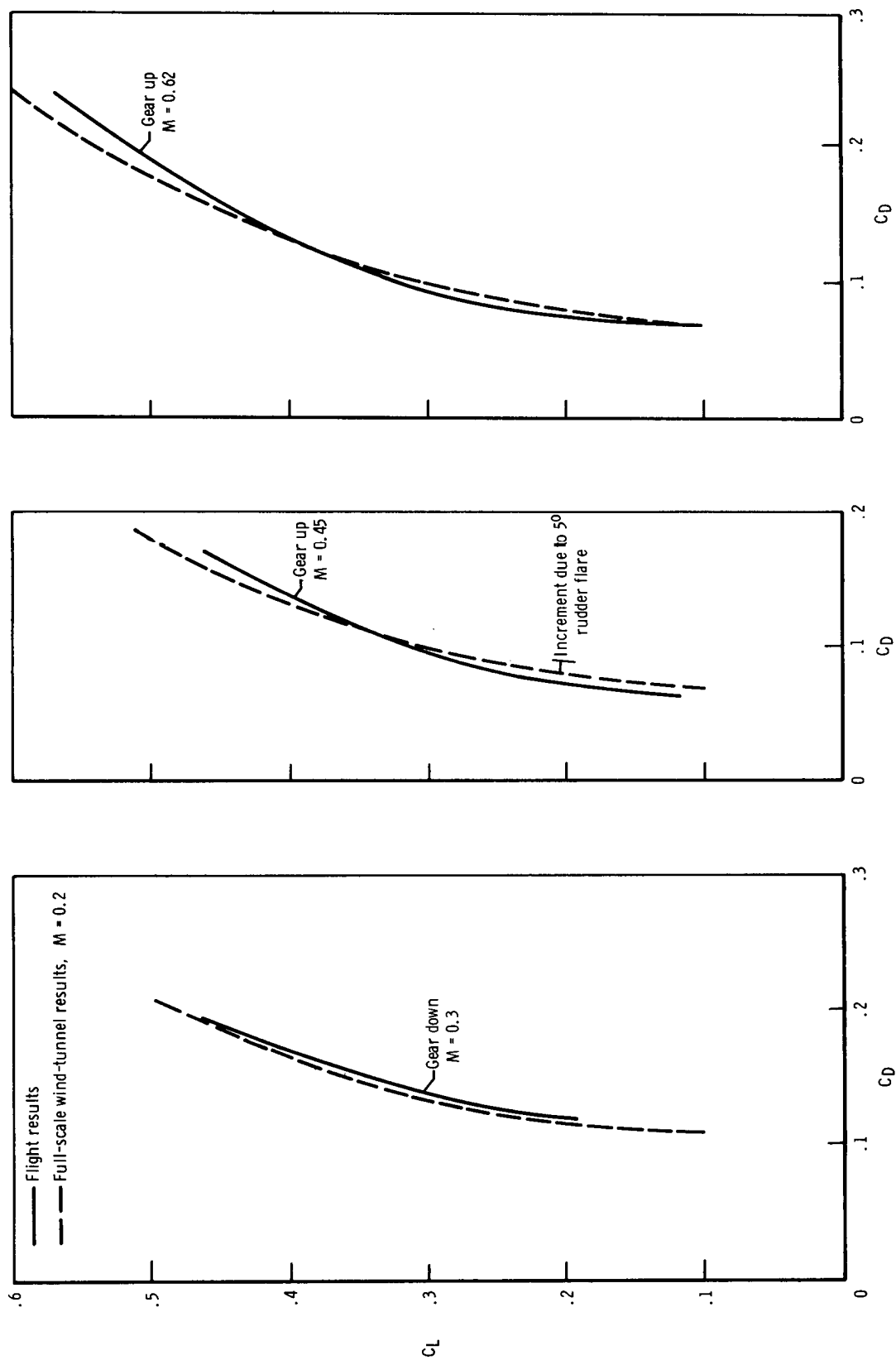
Figure 15.— Comparison of flight M2-F2 drag polars with full-scale wind-tunnel results. $\delta_{uf} = -11.5^{\circ}$.

gear-up flight and wind-tunnel drag results would probably be greater than the comparison presented over most of the C_L range shown. The 5° rudder-flare drag increment is about 7 percent of the unadjusted drag at the lift coefficient of 0.2.

The flight drag results were used to obtain "linearized" drag polars, which are presented with full-scale wind-tunnel results in figure 16. The following table presents the pertinent drag quantities for the figure:

	Gear down		Gear up		
	Flight, M = 0.3	Wind tunnel, M = 0.2	Flight, M = 0.45	Flight, M = 0.62	Wind tunnel, M = 0.2
$C_{D_{min}}$ (extrapolated)	0.110	0.107	0.064	0.063	0.070
$\dfrac{\Delta C_D}{\Delta C_L{}^2}$ *	0.457	0.493	0.500	0.505	0.473

The flight minimum drag coefficients were determined by extrapolating the curves of figure 16 to $C_L = 0$, assuming that the flight curves should have the same shape as the wind-tunnel curves at the lower lift coefficients. The gear-up flight data indicate approximately 10 percent less minimum drag coefficient than the full-scale wind-tunnel prediction and have a greater drag-due-to-lift, shown by a 6 percent greater slope of $\dfrac{\Delta C_D}{\Delta C_L{}^2}$, than the full-scale wind-tunnel data. The gear-down flight results indicate the opposite trends; that is, the flight results have less drag-due-to-lift and slightly higher minimum drag coefficient than the wind-tunnel data.

---

*The values of $\dfrac{\Delta C_D}{\Delta C_L{}^2}$ were derived by assuming that the $C_L{}^2$ versus C_D curve (shown in the sketch) was linear between values of $C_L{}^2$ which correspond to 95 percent of the maximum lift-drag ratio.
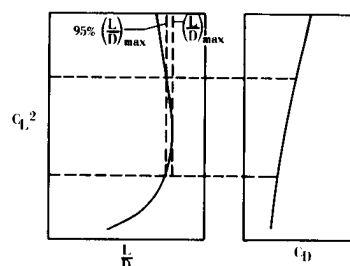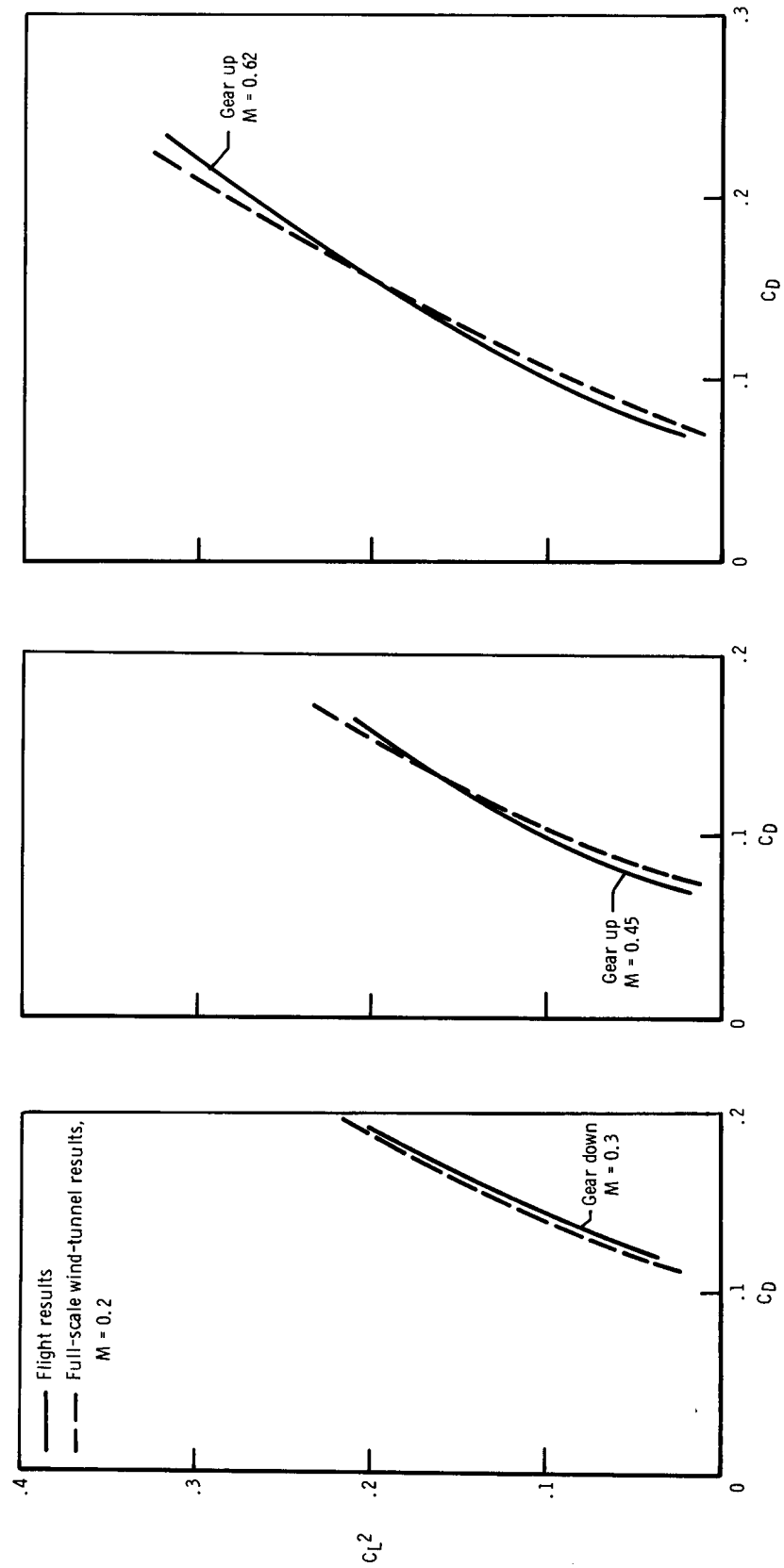
Figure 16.— Linearized drag polars obtained from M2-F2 flight data compared with full-scale wind-tunnel results. $\delta_{uf} = -11.5^o$.

The M2-F2 lift-drag-ratio curves obtained by fairing the flight results (fig. 12) are presented as a function of lift coefficient in figure 17 and compared with full-scale wind-tunnel results. The maximum lift-drag ratios and corresponding quantities from the figure are presented in the following table:

	Gear down		Gear up		
	Flight, $M = 0.3$	Wind tunnel, $M = 0.2$	Flight, $M = 0.45$	Flight, $M = 0.62$	Wind tunnel, $M = 0.2$
$\left(\dfrac{L}{D}\right)_{max}$	2.36	2.41	3.13	3.16	3.07
C_L at $\left(\dfrac{L}{D}\right)_{max}$	0.415	0.425	0.290	0.325	0.350

Very little effect of Mach number is shown for the gear-up flight maximum lift-drag ratios; however, there is a noticeable difference between the lift coefficients at $\left(\dfrac{L}{D}\right)_{max}$. Figure 17 indicates that the vehicle maintains a value of $\dfrac{L}{D}$ within 5 percent of $\left(\dfrac{L}{D}\right)_{max}$ over a significant range of C_L (0.25 to 0.41) which corresponds to angles of attack from 1.5° to 9°. The flight maximum lift-drag ratios are approximately 3 percent higher than the wind-tunnel maximum lift-drag ratios for wind-tunnel results with 0° rudder flare. The effect of adjusting the wind-tunnel results to 5° rudder flare (obtained from limited wind-tunnel data mentioned previously) is shown as an increment of $\dfrac{L}{D}$ (0.17 at $C_L = 0.2$) in figure 17 (M = 0.45). If adequate data were available from which to adjust the wind-tunnel lift-drag-ratio curves, the differences between the flight and wind-tunnel lift-drag ratios would be expected to be greater. The lift coefficients required to attain maximum lift-drag ratios are lower for the gear-up flight results than predicted by the full-scale wind-tunnel tests (see above table). This difference would probably be significant in planning the optimum angle of attack at which a mission vehicle should fly the terminal phase of an entry mission.

As shown in figure 17, extension of the landing gear for the M2-F2 vehicle causes a reduction in the maximum lift-drag ratio of approximately 25 percent. The gear-down flight results indicate fairly good agreement with the full-scale wind-tunnel data. The agreement of the flight and wind-tunnel gear-down data and the differences mentioned for the gear-up data give further evidence of the probable interference of the wind-tunnel mounts on the flight vehicle during the full-scale wind-tunnel tests. As shown in figures 6(a) and 6(b), the gear-up mounting could result in significant interference, whereas the interference from gear-down mounting should be insignificant.
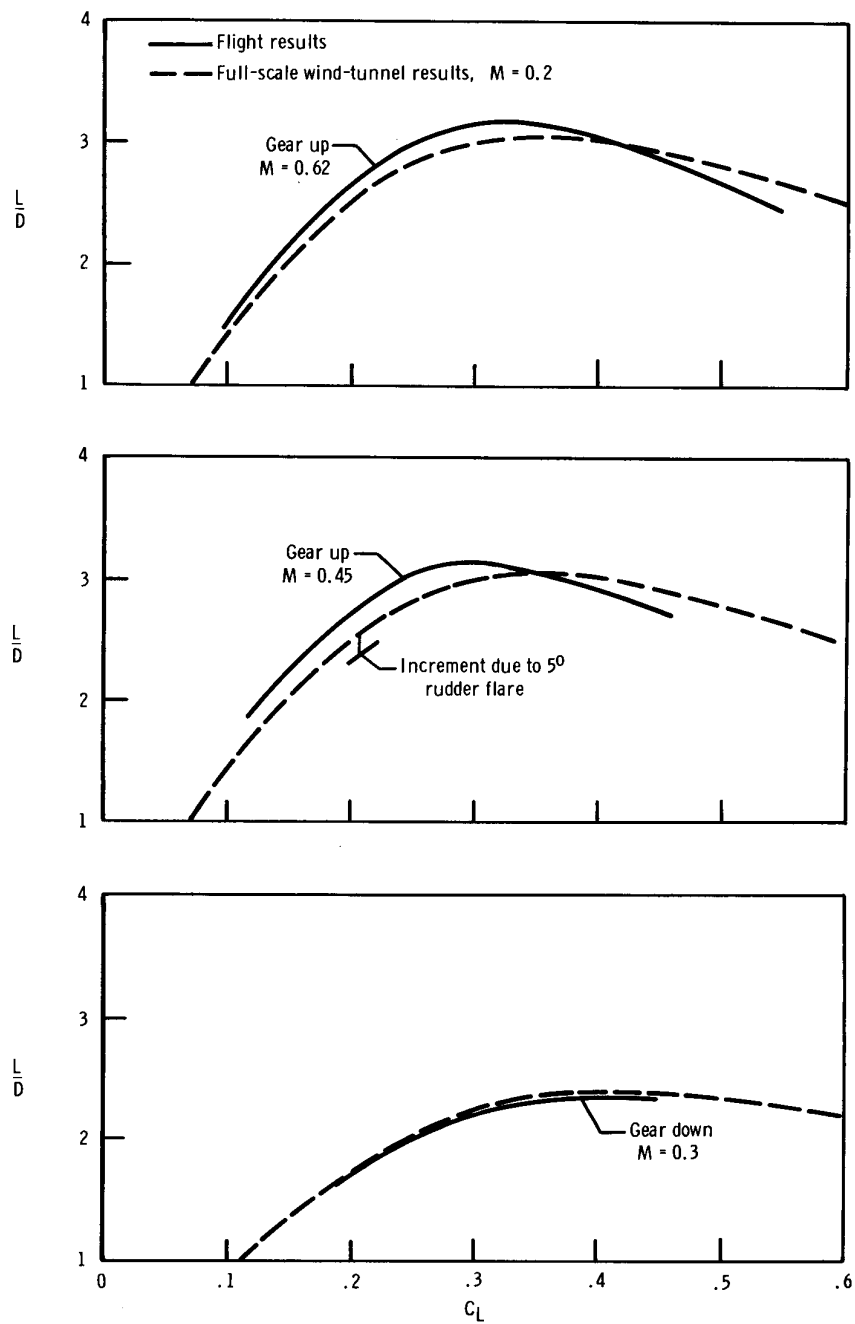
24

Figure 17.— Comparison of M2-F2 lift-drag-ratio data obtained in flight with full-scale wind-tunnel results. $\delta_{uf} = -11.5°$.

Effect of Upper-Flap Deflection

The lift and drag characteristics of the M2-F2 vehicle can be changed by changing the deflection of the upper and lower flaps. As the upper-flap deflection is increased (larger negative deflection) the lower-flap deflection must be increased (larger positive deflection) to maintain trim conditions. The increased deflection of both flaps causes the boattail to become wedge shaped (larger base area) and thus increases the base drag.

The effects of upper-flap deflections of -8.7°, -11.5°, and -14.5° on the M2-F2 flight lift and drag characteristics are shown in figure 18. At a constant lift coefficient of 0.3 (fig. 18(a)), the amount of lower-flap deflection needed to maintain trim flight conditions between upper-flap deflections of -8.7° and -11.5° is double that needed between upper-flap deflections of -11.5° and -14.5°.

The change in wedge angle* from 24° to 31.7° between upper-flap deflections of -8.7° and -11.5° does not significantly alter the lift and drag characteristics (figs. 18(b) to 18(d)). However, the change in wedge angle from 31.7° to 37° between upper-flap deflections of -11.5° and -14.5° increases the drag and thus reduces the lift-drag ratio.

The loss in lift-drag ratio at $C_L = 0.3$ for the larger wedge angles is also shown in figure 19, in which the lift-drag ratios are shown at the three combinations of upper- and lower-flap deflections. The loss of lift-drag ratio is negligible between the upper-flap deflections of -8.7° and -11.5° but increases significantly between the larger upper-flap deflections.

---

*Wedge angles are obtained by adding the absolute deflections (above and below the body contours, δ_{uf} and $\delta_{lf} = 0°$) of the upper and lower flaps at a constant lift coefficient of 0.3.
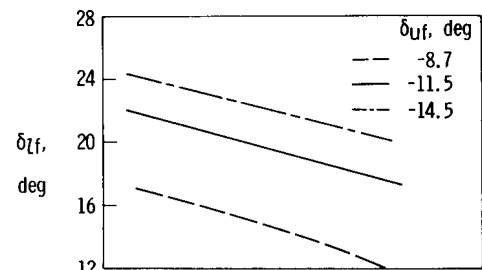
(a) Variation of lower-flap deflection with C_L at constant upper-flap deflection.
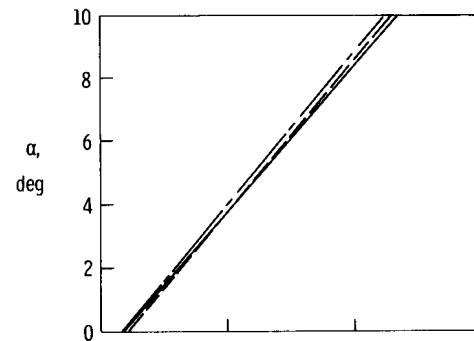
(b) Lift curves.
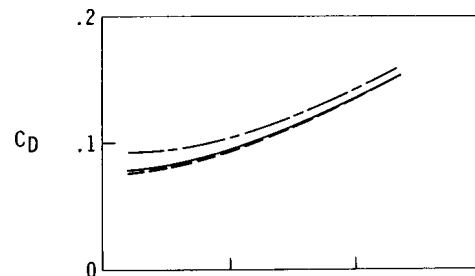
(c) Drag polars.

(d) Lift-drag ratios.

Figure 18.— Effect of upper-flap deflection on the subsonic lift and drag characteristics of the M2-F2. M = 0.62.

26

Figure 19.— Variation of lift-drag ratio with wedge angle for the M2-F2. $C_L = 0.3$;
M = 0.62. (Drawings are exaggerations of actual flap deflections.)

Comparison of M2-F2 and M2-F1 Flight Lift and Drag Characteristics

As previously discussed, the M2-F2 configuration is a follow-on version of the M2-F1 configuration tested earlier; therefore, it is of interest to compare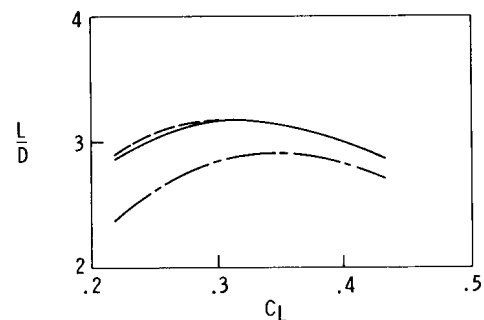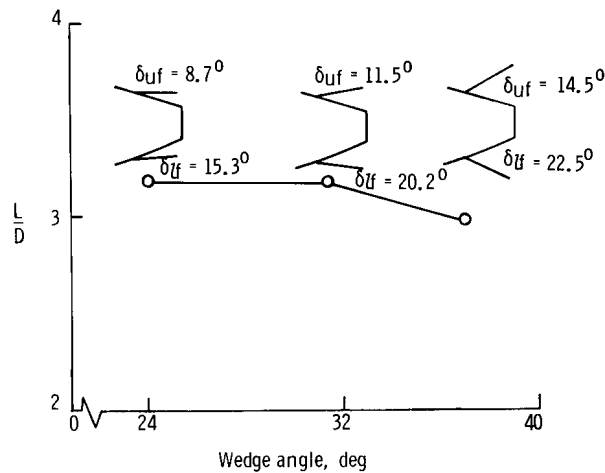 test results from these vehicles. However, the heavyweight M2-F2 lifting body is significantly different from the original M2-F1 configuration (ref. 5). A three-view drawing of the M2-F1 is shown in figure 20. Although the basic M-2 13° blunted half-cone body was utilized for both vehicles, the canopy placement, landing-gear systems, and control surfaces were changed. The M2-F1 vehicle had a fixed landing-gear assembly that protruded from the hull of the vehicle and did not include the large wheel-well cavities of the M2-F2 configuration. The M2-F1 canopy was much farther rearward than on the M2-F2 vehicle. The M2-F1 body was shorter, with the control flaps and rudders extending beyond the base of the vehicle. The elevons were outboard of the vertical stabilizers and were used in conjunction with the trailing flaps for pitch and roll control. This vehicle did not have a lower flap for longitudinal control as does the M2-F2 vehicle.
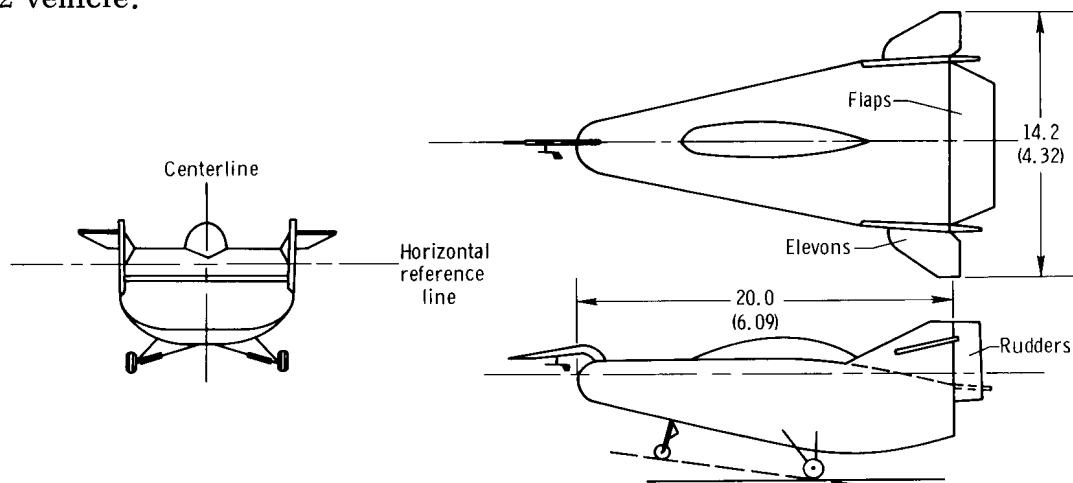

Figure 20.— Three-view drawing of the M2-F1 configuration. All dimensions in feet (meters).

27

Lift and drag characteristics of the vehicles are compared in figure 21. As can be seen in figure 21(a), the lift-curve slopes are different. The M2-F2 vehicle has a greater drag coefficient and less lift-drag ratio than the M2-F1 (figs. 21(b) and 21(c)), caused primarily by the drag penalty associated with an extendable landing-gear system. (The landing-gear system of the M2-F2 is described in the VEHICLE DESCRIPTION section.) The actual projected body lifting surface areas of the vehicles differ (M2-F1 is approximately 10 feet^2 (0.929 meter^2) larger than the M2-F2) and have significant effect on the comparison of lift and drag characteristics of the vehicles. In view of the many configuration differences between the two vehicles, the agreement obtained was as good as could be expected.
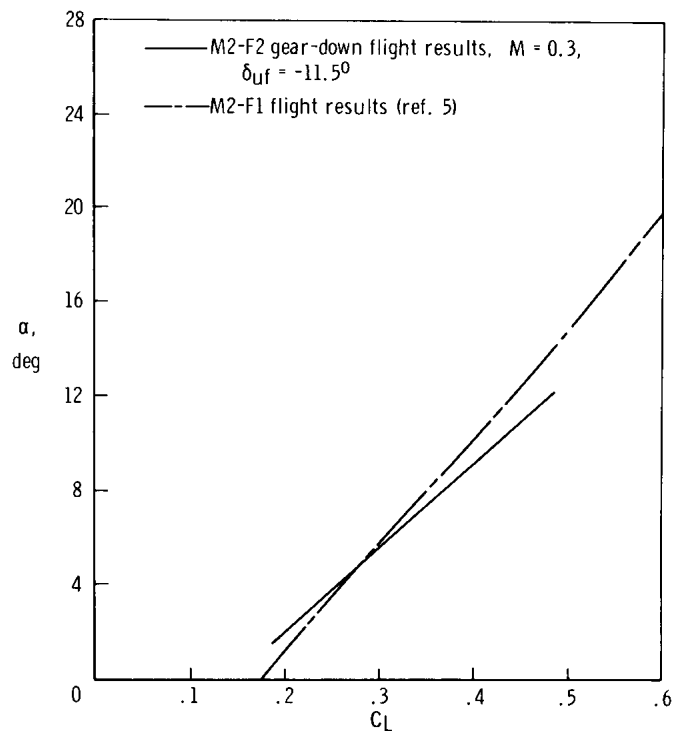
(a) Lift curve.
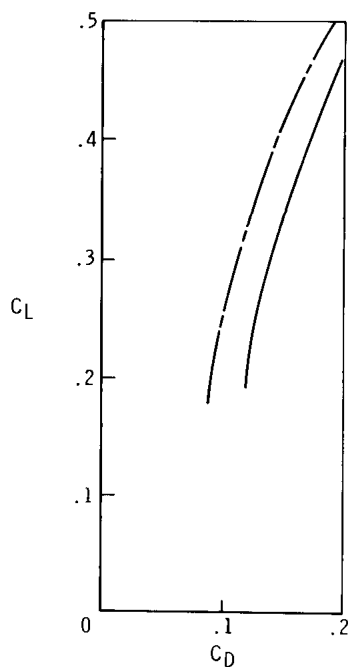
(b) Drag polars.
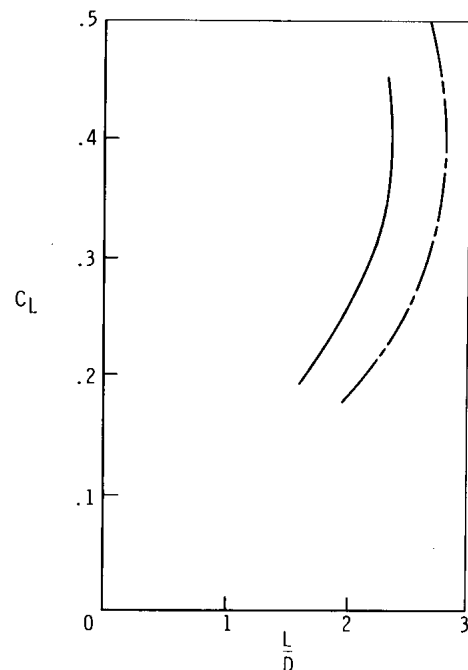
(c) Lift-drag ratios.

Figure 21.— Comparison of the lift and drag characteristics for the M2-F2 and M2-F1 configurations.

28

CONCLUSIONS

The lift and drag characteristics of the M2-F2 lifting-body configuration obtained during subsonic gliding flight indicated that:

1. Ninety-five percent of the maximum lift-drag ratio (3.13 to 3.16, gear up) is available through an angle-of-attack range of 1.5° to 9° at an upper-flap deflection of -11.5°.

2. The extension of the landing gear on the M2-F2 vehicle causes a loss of approximately 25 percent in maximum lift-drag ratio.

3. The gear-up flight and full-scale wind-tunnel maximum lift-drag ratios agree within 3 percent; however, the wind-tunnel data were obtained at a rudder-flare deflection of 0° and the flight results are for a rudder-flare deflection of 5°. The difference between flight and wind-tunnel results would probably be greater than shown if the wind-tunnel data had been adjusted for the 5° flare.

4. The lift coefficient required to attain maximum lift-drag ratios is lower for the gear-up flight results than predicted by the full-scale wind-tunnel tests.

Flight Research Center,
    National Aeronautics and Space Administration,
        Edwards, Calif., April 14, 1967,
            727-00-00-01-24.

REFERENCES

1. Dennis, David H.; and Edwards, George G.: The Aerodynamic Characteristics of Some Lifting Bodies. NASA TM X-376, 1960.

2. Kenyon, George C.; and Edwards, George G.: A Preliminary Investigation of Modified Blunt 13° Half-Cone Re-Entry Configurations at Subsonic Speeds. NASA TM X-501, 1961.

3. Rakich, John V.: Aerodynamic Performance and Static-Stability Characteristics of a Blunt-Nosed, Boattailed, 13° Half-Cone at Mach Numbers From 0.6 to 5.0. NASA TM X-570, 1961.

4. Kenyon, George C.; and Sutton, Fred B.: The Longitudinal Aerodynamic Characteristics of a Re-Entry Configuration Based on a Blunt 13° Half-Cone at Mach Numbers to 0.92. NASA TM X-571, 1961.

5. Horton, Victor W.; Eldredge, Richard C.; and Klein, Richard E.: Flight-Determined Low-Speed Lift and Drag Characteristics of the Lightweight M2-F1 Lifting Body. NASA TN D-3021, 1965.

6. Mechtly, E. A.: The International System of Units - Physical Constants and Conversion Factors. NASA SP-7012, 1964.

7. Matranga, Gene J.: Analysis of X-15 Landing Approach and Flare Characteristics Determined From the First 30 Flights. NASA TN D-1057, 1961.

8. Larson, Terry J.; and Webb, Lannie D.: Calibrations and Comparisons of Pressure-Type Airspeed-Altitude Systems of the X-15 Airplane From Subsonic to High Supersonic Speeds. NASA TN D-1724, 1963.

9. Beeler, De E.; Bellman, Donald R.; and Saltzman, Edwin J.: Flight Techniques for Determining Airplane Drag at High Mach Numbers. NACA TN 3821, 1956.

10. Yaggy, Paul F.: A Method for Predicting the Upwash Angles Induced at the Propeller Plane of a Combination of Bodies With an Unswept Wing. NACA TN 2528, 1951.

11. Zalovcik, John A.: A Radar Method of Calibrating Airspeed Installations on Airplanes in Maneuvers at High Altitudes and at Transonic and Supersonic Speeds. NACA Rep. 985, 1950.

TABLE I.— PHYSICAL CHARACTERISTICS OF THE M2-F2 VEHICLE

Body —
  Area:
    Planform, feet^2 (meters^2) 160 (14.9)
    Planform, reference, feet^2 (meters^2) 139 (12.9)
  Length, feet (meters) 22.2 (6.76)
  Span, feet (meters) 9.95 (3.033)
  Aspect ratio, basic vehicle:

$$\frac{b^2}{S} \quad \text{. . . . . } \quad 0.619$$

$$\frac{b^2}{S}, \text{ reference area} \quad \text{. . . . . } \quad 0.712$$

  Weight, including pilot, pounds (kilograms) 6000 (2722)
  Center of gravity, percentage of body length 49
  Wetted surface area, feet^2 (meters^2) 471 (43.8)
  Base area, feet^2 (meters^2) 9.63 (0.895)
  Basic body cone angle, degrees 13
Lower flap —
  Area, feet^2 (meters^2) 15.53 (1.443)
  Span, feet (meters) 5.40 (1.646)
  Chord, feet (meters) 2.88 (0.876)
  Flap travel, down, degrees . . . . 0 to 35
Upper flaps —
  Area, each, feet^2 (meters^2) 9.72 (0.903)
  Span, each, feet (meters) 4.28 (1.307)
  Chord, feet (meters) 2.27 (0.691)
  Symmetric travel, up, degrees . . . . 0 to -35
  Asymmetric travel, degrees . . . . ±15
Vertical stabilizers, two —
  Area, each, feet^2 (meters^2) 16.10 (1.496)
  Height, trailing edge, feet (meters) 3.79 (1.16)
  Chord, feet (meters):
    Root 7.36 (2.24)
    Tip 2.58 (0.79)
  Leading-edge sweep, degrees 62
  Base area, each, including rudders, feet^2 (meters^2) 0.83 (0.08)
Rudders, two —
  Area, each, feet^2 (meters^2) 5.97 (0.555)
  Height, each, feet (meters) 4.78 (1.457)
  Chord, feet (meters) 1.25 (0.381)
  Travel, outward, degrees . . . . 0 to 45
  Base area, each, feet^2 (meters^2):
    Open, 5° flare 1.02 (0.0948)
    Closed 0.51 (0.047)